Available online www.jocpr.com

Journal of Chemical and Pharmaceutical Research, 2017, 9(4):171-179

Research Article

ISSN : 0975-7384
CODEN(USA) : JCPRC5

Spectroscopic Studies and Thermal Analysis on Cefoperazone Metal Complexes

Mamdouh S Masoud[1], Alaa E Ali[2*], Gehan S Elasala[2] and Sherif A Kolkaila[2]

[1]*Chemistry Department, Faculty of Science, Alexandria University, Egypt*
[2]*Chemistry Department, Faculty of Science, Damanhour University, Egypt*

ABSTRACT

*The metal complexes of cefoperazone with transition metals (Cr(III), Mn(II), Fe(III), Co(II), Ni(II), Cu(II), Zn(II), Cd(II) and Hg(II)) were synthesized. From IR spectra proved that cefoperazone acts as bidentate ligand. The active sites for coordination of cefoperazone were confirmed by using the hyper-chemistry program. The magnetic measurement and spectral data proved octahedral structure for all complexes except that of Ni, Cu and Hg, those have tetrahedral structural. The thermal decomposition mechanisms of the prepared complexes were studied and suggested. The kinetic and thermodynamic parameters of the thermal decomposition steps, Ea, ΔH*and ΔS*, were estimated from DTA thermograms. Cefoperazone complexes showed higher activity than commercial cefoperazone for some strains.*

Keywords: Cephalosporins complexes; Cefoperazone; Thermal analysis; Biological screening

---

INTRODUCTION

Cephalosporins are classified to five generations according to antimicrobial activity where the later generations have greater activity towards Gram-negative bacteria than older generations [1]. The role of cephalosporins is inhibition of bacterial cell-wall synthesis. Production of betalactameses can damage the betalactam ring and make cephalosporins inactive [2]. Cefoperazone (Figure 1) is a third generation cephalosporin antibiotic, which has higher activity towards gram negative and lower activity towards gram positive. Cefoperazone is marketed under brand names cefobid and cefrone.

Cefoperazone is characterized by higher efficacy in treating Pseudomonas bacterial infections. Also cefoperazone is used for treating infections of the respiratory and urinary tract. Previous work in cefoperazone metal complexes fell to synthesis cefoperazone complexes with (Cr, Mn, Zn and Hg) [3]. The complexion properties, thermal behavior and antibacterial activity of cefoperazone and their metal complexes are discussed. Cefoperazone can form five-membered ring with metal ion during formation of complexes which give high stability for the synthesized complexes. From DTA and TG curves the mechanism of decomposition is explained and the thermodynamic parameters are evaluated and discussed.

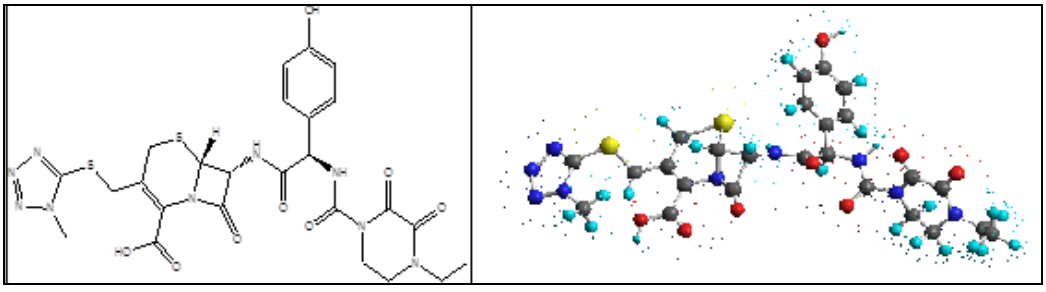

Figure 1: Structure of Cefoperazone (HL)

EXPERIMENTAL SECTION

Cefoperazone (standard pure drug) was obtained from the Egyptian company Epico. All complexes were synthesized by dissolving the metals [Cr(III), Mn(II), Fe(III), Co(II), Ni(II), Cu(II), Zn(II), Cd(II) and Hg(II)] as metal chlorides in 40 ml ethanol. Cefoperazone was dissolved in 40 ml bidistilled water. The prepared solution of cefoperazone was mixed with each ethanolic solution of each metal chloride with molar ratio 1:1. The reaction mixture was refluxed for about 5 min then left over-night; coloured products precipitated and were isolated by filtration. The products were washed with water and EtOH-H_2O and dried in a vacuum desiccator over anhydrous $CaCl_2$. The analytical studies (Table 1) of all the synthesized complexes were done by the usual methods [4]. The metal contents were determined based on atomic absorption technique using model 6650 Shimadzu-atomic absorption spectrophotometer and complexometrically with standard EDTA solution using the appropriate indicator as reported [5]. The analysis of chloride contents of the complexes were determined by applying the familiar Volhard method [6]. The proposed structures of synthesized metal complexes were illustrated in Figure 2.

Physical Measurements

IR spectra of the cefoperazone and their metal complexes were recorded on Perkin Elmer spectrophotometer, Model 1430 which it is range of 200-4000 cm^{-1}. Spectra of cefoperazone and the solid complexes were measured in Nujol mull spectra by use Unicam UV/Vis spectrometer [7]. The correction of Molar magnetic susceptibilitiesby using Pascal's constants were determined at room temperature (298 K) using Faraday's method. ESR spectra were recorded on reflection spectrometer operating at (9.1–9.8) GHZ in a cylindrical resonance cavity with 100 KHZ modulation. The g values were determined by comparison with DPPH signal. Differential thermal analysis (DTA) and thermogravimetric analysis (TGA) of the ligand (cefoperazone) and their complexes were recorded on Shimadzu DTA/TGA-60 thermal analyzer with heating rate 20°C/min under nitrogen atmosphere of flow rate 20 ml/min. The biological screening of cefoperazone and their metal complexes were examined against 5 microorganisms representing different microbial categories, {two Gram-positive (*Staphylococcus Aureas* ATCC6538P and *Bacillus subtilis* ATCC19659), two Gram negative (*Escherischia coli* ATCC8739 strain and *Pseudomonas aeruginosa* ATCC9027) and candida albicans as a fungi. Hyperchem computer program using PM3 semi-empirical and Molecular Mechanics Force Field (MM+) is applied for ligand.

Table 1: Elemental analysis, m.p., formula, stoichiometries and colour of cefoperazone complexes

Complexes	Colour	Calculated (Found)%					
		C	H	N	S	M	Cl
[CrL(OH)(Cl)(H_2O)$_2$]	Violet	39.12 (39.95)	4.04 (4.22)	15.79 (14.94)	8.03 (7.7)	6.51 (6.32)	4.44 (4.73)
[Mn L(HL)Cl(H_2O)]	Yellow	41.36 (41.44)	4.71 (4.42)	17.22 (17.82)	7.89 (7.72)	6.76 (6.37)	4.37 (4.73)
[Fe(HL)LCl_2]	Dark brown	42.42 (42.5)	3.7 (3.72)	17.8 (17.81)	9.06 (9.12)	3.94 (3.97)	5.01 (5.06)
[CoL(HL)Cl(H_2O)]	Pink	41.74 (41.92)	5.14 (5.51)	16.23 (16.12)	7.43 (7.11)	6.83 (6.13)	4.11 (4.99)
[NiLCl(H_2O)]	Indigo	40.41 (40.11)	4.17 (4.16)	16.31 (16.12)	8.3 (8.62)	7.59 (7.6)	4.59 (4.7)
[CuLCl(H_2O)]	Green	33 (38.11)	4.58 (4.62)	14.08 (14.01)	6.78 (6.71)	13.43 (13.44)	3.75 (3.65)
[ZnLCl(H_2O)]	Yellow	39.33 (39.22)	3.7 (3.41)	16.51 (16.77)	8.4 (8.55)	8.56 (8.44)	4.46 (4.73)
[Cd L(HL)Cl(H_2O)]	Yellow	35.72 (35.1)	3.36 (3.45)	16.66 (16.12)	7.37 (7.12)	13.37 (14.73)	4.22 (4.22)
[HgLCl(H_2O)]	White	33.41 (33.42)	3.14 (3.15)	14.03 (14.01)	7.14 (7.15)	22.32 (22.31)	3.94 (3.95)

All the complexes have m.p > 300º C

RESULTS AND DISCUSSION

The assignments of bonding sites of cefoperazone and their metal complexes were summarized in Table 2. All the prepared complexes contain water except complex of Fe(III). In general, water in inorganic salts may be classified as lattice or coordinated water. Generally, lattice water absorbs at 3550-3200 cm^{-1} (asymmetric and symmetric OH stretching) [8]. Cefoperazone complexes showed broad bands in the 3400 – 3580cm^{-1} region in all prepared complexes suggesting coordination with water except Fe. It seems from the elemental analysis of the complexes and thermal analysis that all complexes contain water molecules in their structures. This is evident by ν_{OH}. However, coordinated water in these complexes is indicated by the appearance of metal-oxygen bands attributable to rocking modes at 422-450 cm^{-1} region [9]. The band of N-H stretching vibration appears at 3425 cm^{-1} in spectra of cefoperazone. Generally the ring carbonyl absorption frequency will be shifted to higher wave numbers as the ring becomes more and more strained. The lactam (C=O) band appears at 1770 cm^{-1} in the spectrum of cefoperazone which is shifted in the simple complexes spectra (1776 - 1787cm^{-1}) range. The amide C=O-NH band appears at 1677 cm^{-1} in the spectrum of cefoperazone while the complexes show this band at 1674 - 1675 cm^{-1}, suggesting that ligand coordination with these metal ions occurs through the oxygen from the lactam carbonyl group rather than the amide carbonyl group, where the shifting was not significant. The band due to ν_{C-N}

of β-lactam ring (1461cm^{-1}) and ν_{C-O} of methoxy group (1101 cm^{-1}) in the free ligand remain unchanged on complexation. The band at 1610.09 cm^{-1}, corresponding to the carboxylate asymmetrical stretching of the free ligand, is shifted (1- 4 cm^{-1}) to higher wave numbers in the spectra of the complexes indicating coordination through this group [10]. A carboxylate ligand can bind to the metal either monodentate or bidentate, giving changes in the relative positions of the antisymmetric and symmetric stretching vibrations [11]. The IR spectra of the complexes give a separation value of more than 200 cm^{-1} suggesting monodentate carboxylate. The remaining carboxylate bands ν_{COO} (symm), γ (COO), ρ(COO) and ω(COO), formerly at 1364.33, 756, 609.76 and 530.00 cm^{-1} , respectively, the change in position is a result of coordination. The ν_{C-O} band observed at 1513.35 cm^{-1} in free cefoperazone appears at 1513 cm^{-1} in the metal complexes so that, the shifting was not significant. In the far IR spectra, the bonding of nitrogen and oxygen is provided by the presence of bands at 450.37 cm^{-1} (M-N) and 464.22-495.61 cm^{-1} (M-O) [12].

Table 2: Fundamental infrared bands (cm^{-1}) of cefoperazone and its metal complexes

Compound	ν_{NH}	$\nu_{C=O}$ lactam	$\nu_{C=O}$ amide	ν_{COO} asym	ν_{COO} sym	ν_{C-N} of β-lactam	ν_{C-O} stretch	ν_{M-N}	ν_{M-O}	ν_{M-Cl}
Cefoperazone	3425	1770	1677	1610	1364	1461	1011	-	-	-
[CrL(OH)(Cl)(H$_2$O)$_2$]	3290	1776	1674	1615	1364	1460	1012	534	435	343
[Mn L(HL)Cl(H$_2$O)]	3298	1767	1675	1615	1365	1461	1013	524	440	342
[Fe(HL)LCl$_2$.]	3295	1782	1675	1615	1365	1461	1015	523	442	350
[CoL(HL)Cl(H$_2$O)]	3392	1776	1676	1615	1365	1462	1011	523	430	360
[NiLCl(H$_2$O)]	3293	1778	1675	1615	1366	1462	1012	524	432	362
[CuLCl(H$_2$O)]	3428	1758	1657	1614	-	1461	1018	523	450	362
[ZnL Cl (H$_2$O)]	3296	1782	1675	1615	1387	1461	1017	491	423	392
[Cd L(HL)Cl (H$_2$O)]	3297	1782	1675	1615	1368	1462	1019	524	427	377
[HgLCl(H$_2$O)]	3284	1787	1674	1613	1365	1460	1012	525	422	342

Electronic Spectral and Magnetic Studies

The electronic absorption spectra for the violet chromium-complex, [CrL(OH)(Cl)(H$_2$O)$_2$] had three bands at 278, 410, 547 nm due to $^4A_{2g}\rightarrow{}^4T_{2g}$ (F), $^4A_{2g}\rightarrow{}^4T_{1g}$(F) and $^4A_{2g}\rightarrow{}^4T_{1g}$(p) transitions, respectively, (Table 3). So the complex has octahedral geometries. Such Oh geometry is further deduced from the μeff values which equals, 3.40 B.M, respectively [13]. However, the yellow electronic absorption spectrum of manganese-complex, [Mn L(HL)Cl(H$_2$O)], (Table 3), had three bands , 424.8, 446.2, 693.2 where the first band is assigned to $^6A_{1g}\rightarrow{}^4A_{1g}$, while the second is due to $^6A_{1g}\rightarrow{}^4T_{2g}$ transition and the last band is due to $^6A_{1g}\rightarrow{}^4T_{1g}$ transition. Its room temperature μeff value of 4.92 and, typified the existence of Oh configuration. The brown electronic absorption spectra of iron-complex, [Fe(HL)LCl$_2$.], (Table 3), had bands at 357, 422, 518 nm,. These bands are due to CT ($t_{2g}\rightarrow\pi^*$) and CT ($\pi\rightarrow e_g$) with μ_{eff} value of 5.9, typified the existence of *Oh* configuration. The electronic absorption spectra of [CoL(HL)Cl(H$_2$O)], (Table 3), gave bands at 278, 410, 542, nm. Bands are of charge transfer nature and the latter broad bands are assigned to $^4T_{1g}$(F) → $^4T_{2g}$(P) transition with magnetic moment value equal to 5.85 typified the existence of the complex in Oh geometry for cefoperazone [14]. The green electronic absorption spectra for Nickel-complex, [NiLCl(H$_2$O)] showed three bands at 248, 426, 638 nm due to π - π*, $^3T_1$(F)→$^3T_1$(P) and $^3T_1$(F)→$^3A_2$ transitions, respectively (Table 3).

Table 3: Nujol mull electronic absorption spectra λ_{max} (nm), room temperature effective magnetic moment values (μ_{eff} 298°K) and geometries of cefoperazone metal complexes

Complex	λ_{max} (nm)	μ_{eff}	Geometry
[CrL(OH)(Cl)(H$_2$O)$_2$]	278,410, 547	3.4	O_h
[Mn L(HL)Cl(H$_2$O)]	205, 424, 446, 693	4.92	O_h
[Fe(HL)LCl$_2$.]	357, 422, 518	5.7	O_h
[CoL(HL)Cl(H$_2$O)]	301, 426, 516	5.85	O_h
[NiL Cl(H$_2$O)]	248, 426, 638	2.78	T_d
[CuLCl(H$_2$O)]	254, 425	1.75	T_d
[ZnL Cl (H$_2$O)]	427	diamagnetic	T_d
[Cd L(HL)Cl (H$_2$O)]	335	diamagnetic	O_h
[HgLCl(H$_2$O)]	344	diamagnetic	T_d

So the complex has tetrahedral geometries, further deduced from the μeff values which equals, (2.78) B.M. The copper complex,[CuLCl(H$_2$O)] (Table 3), exhibited bands at 245, 425 nm cefoperazone complexes showed two bands at 245 and 435.6 nm with μeff=1.73 B.M. The latter broad band is assigned to the $^2E_g\rightarrow{}^2T_{2g}$ (D) transition assignable to octahedral environment [14,15]. Zn, Hg and Cd complexes exhibited only a high intensity band at 329-365 nm, which are assigned to ligand →metal charge transfer. Owing to the d10-configuration of Zn(II), Cd(II) and Hg(II), no d-d transition could be observed and therefore the sterochemistry around these metals in its complexes can be hardly determined.

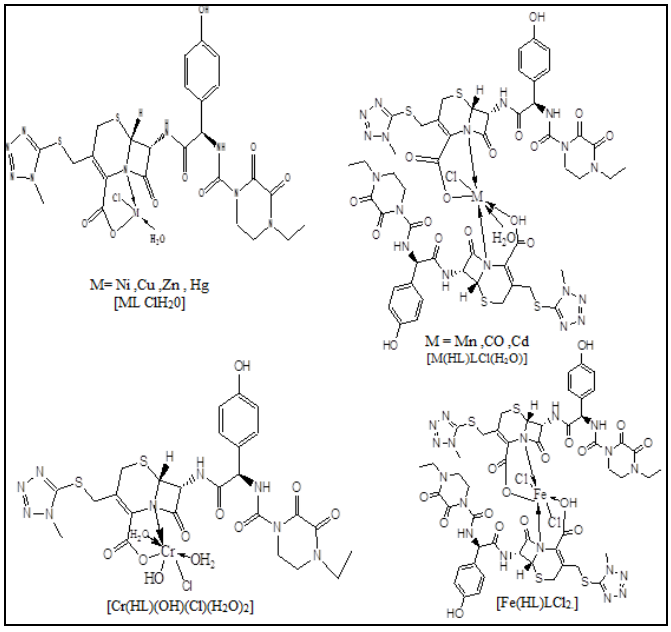

Figure 2: Proposed structures of cefoperazone complexes

From hyper-chem program charge density of cefoperazone atoms is calculated, Figure 3 confirmed cefoperazone coordination through the carboxylates, which has highest charge.

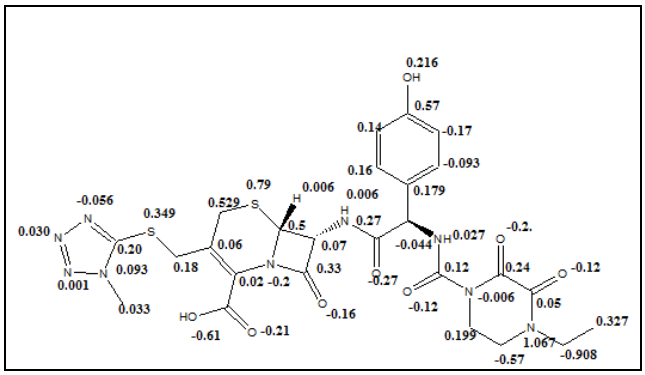

Figure 3: Charge density of cefoperazone atoms

Electron Spin Resonance of Copper Complex

The room temperature polycrystalline X-band ESR spectral pattern of [CuLCl(H_2O)] complex, Figure 4 is axial compressed nature. The spectral analysis of this complex gave two g values g_{11}= 2.25 and g_1= 2.015. The calculated <g> value=2.17. While the low value of f^2 shows strong axial field.

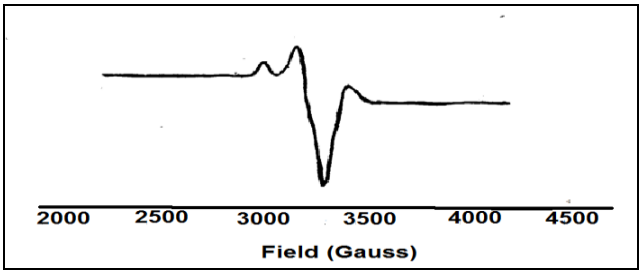

Figure 4: ESR of [CuLCl(H_2O)]

RESULTS AND DISCUSSION

Biological Activity

In this study, 5 microorganisms representing different microbial categories, {two Gram-positive (*Staphylococcus Aureas* ATCC6538P and *Bacillus subtilis* ATCC19659), two Gram negative (*Escherischia coli* ATCC8739 strain and *Pseudomonas aeruginosa* ATCC9027) bacteria were used. The study included,

cefoperazone and 2 complexes of different metal ions (Zn and Cu)} which are applicable for human person. Two different broadly antibiotics (Ciprofloxacin *and* Clotrimazole) are used in this study as references. Table 4 allows the following observations and conclusions:

All the investigated compounds have higher positive antibacterial activity compared to antifungal activity. [CuLCl(H_2O)] showed similar activities for *Pseudomonas aeruginosa* and *Escherischia coli*. While it have higher activity to, Candida albicans, *Staphyllococcus aureus and Bacillus subtilis*. It revealed by the diameter of its inhibition zone. On the other hand, [ZnLCl(H_2O)] complex showed higher activity to *Escherischia coli*, Candida albicans and *Bacillus subtilis*. It showed activity in the same range of cefoperazone for *Pseudomonas aeruginosa*.

Most of the metal complexes have higher activity than the free ligands such increased activity of the metal chelates could be explained on the bases of overtoneś concept and chelation theory [16]. The cell permeability the lipid membrane that surrounds the cell favours the passage of only lipid soluble materials on the basis that liposolubility is an important factor that controls antimicrobial activity. On chelation, the polarity of the metal ion is reduced to a greater extent due to the overlap of the ligand orbital and partial sharing of the positive charge of the metal ion with the donor groups. Further, it increases the delocalization of p- and d-electrons over the whole chelate and enhances the lipophilicity of the complex. The increased lipophilicity enhances the penetration of the complexes into lipid membranes and blocking of metal binding sites on the enzymes of the microorganism.

Table 4: The antifungal activity of the free cefoperazone and its complexes against some reference strains expressed in absolute activity (AU)

Complexes	Blank	*Candida albicans*	*Escherischia coli*	*Pseudomonas aeruginosa*	*Staphyllococcus aureus*	*Bacillus subtilis*
[CuLCl(H_2O)]	8	14	12	8	12	11
[ZnLCl(H_2O)]	8	16	14	8	14	17
Cefoperazone	8	12	12	8	12	11
Ciprofloxacin	9	30	30	30	30	-
Clotrimazole	10	-	-	-	-	17

Thermal Analysis

The thermal behavior of some biologically active compounds has been reported from Masoud et al. [17-20]. The thermal behavior of was investigated by thermograms (TG and DTA), Figure 5 and the corresponding thermal analysis data is presented in Table 5. In case of cefoperazone, the decomposition occurs in four exothermic steps 50-600°C range. There is no mass loss up to 200°C. The first stage of decomposition starts at 22°C and ends at 200°C with a corresponding weight loss 10.1%, Which is accompanied by exothermic effect in the DTA curve. The second stage of decomposition is observed at 201-288°C (43.43% wt loss). Meanwhile the DTA curve exhibits exothermic effect in the range 210°C which is accompanied by weight loss confirming. The third stage of decomposition starts at 289°C and ends at 496°C with a corresponding weight loss 67.41% which is accompanied by exothermic effect in the DTA curve. The last stage of decomposition start at 497°C and ends at 400°C (94.61% wt loss) Meanwhile the DTA curve exhibits exothermic effect in the range 210°C which is accompanied by confirmed weight loss. The suggested mechanism is given in Scheme 1.

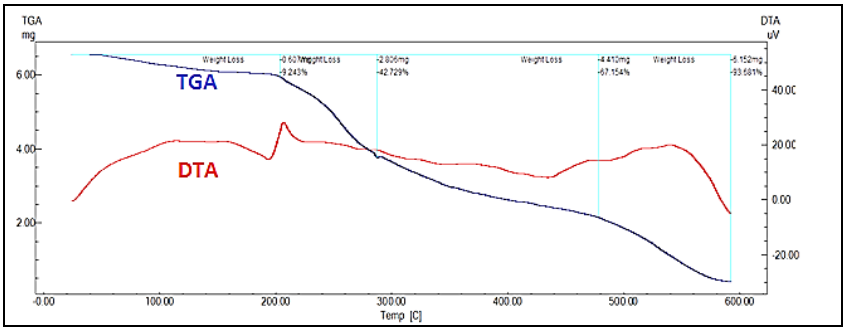

Figure 5: TGA and DTA of cefoperazone ligand

In case of [CrL(OH)(Cl)(H_2O)$_2$] complex, (Figure 6) there is no mass loss up to 36°C. The first stage of decomposition starts at 36°C and ends at 206°C with a corresponding weight loss 11.11%, which is accompanied by endothermic effect in the DTA curve in the range 112.8°C assigned by confirmed weight loss. The second stages of decomposition were observed at 207-400°C (54.87% wt loss). Meanwhile, the DTA curve exhibits exothermic effect in the range 260°C which are accompanied byconfirmed weight loss. The last stage of decomposition start at 401°C and ends at 502°C (90.29% wt loss) meanwhile the DTA curve exhibits exothermic effect in the range 471.5°C as supported by confirmed weight loss. The suggested mechanism is given in Scheme 2.

Table 5: DTA analysis of cefoperazone and its metal complexes

Compound	Type	Tm (°C)	E_a kJ mol^{-1}	n	α_m	$\Delta S^{\#}$ kJ K^{-1} mol^{-1}	$\Delta H^{\#}$ kJ mol^{-1}	Z S^{-1}	Temp. (°C) TGA	Wt. Loss %		Assignment
										Calc	Found	
Cefoperazone	Exo	110	6.34	1.17	0.6	-0.29	-32.6	0.006	22-200°C	9.24	10.1	loss of $2CHN_4$
	Exo	210	294.49	1.16	0.6	-0.27	-57.9	0.168	200-288°C	42.79	43.34	Loss of $6NH_3$, $4CH_3OH$, 2 CH_3COCH_3
	Exo	377.5	158.77	1.74	0.52	-0.29	-109.7	0.05	288-496°C	67.15	67.41	Loss of $6CH_3OH$, $2CH_3SH$,4 NH_3
	Exo	541	47.02	0.94	0.64	-0.3	-166	0.01	496-591°C	93.68	94.61	Loss of $2NH_3$, 2 CH_3COCH_3, $2C_6H_6$, C_4H_{10}.
[CrL(OH)(Cl)(H_2O)$_2$]	Endo	122.8	24.049	1.38	0.57	-0.28	-35.3	0.023	36-206°C	10.47	11.11	Dehydration of $2H_2O$ and loss of $2CHN_4$
	Exo	260	31.685	1.18	0.6	-0.29	-77.4	0.014	206-400°C	54.25	54.78	Loss of $2C_6H_6O$, 8 NH_3, $2CH_3OH$,$2CH_3COCH_3$
	Exo	471.5	66.501	1.11	0.61	-0.3	-142.2	0.016	400-502°C	90.23	90.29	Decomposition of the rest ligand and formation of Cr_2O_3
[Mn L (cefoperazone) Cl(H_2O)]	Endo	142.8	11.7	1.23	0.59	-0.29	-42.3	0.009	26-77°C	1.56	1.28	Dehydration of H_2O
	Exo	255.3	81.6	1.36	0.57	-0.28	-74	0.038	77-199°C	13.99	13.46	loss of $2CHN_4$ and$2NH_3$
	Exo	391.5	82.482	0.77	0.67	-0.29	-116.2	0.025	199-266°C	29.3	29.69	Loss of $2C_6H_6O$ and HCl
	Exo	451.5	240.665	1.95	0.5	-0.29	-131	0.064	266-544°C	64.41	64.21	Loss of $6NH_3$, $6CH_3COCH_3$ and CH_3OH
	Exo	554.4	439.303	1.91	0.5	-0.28	-160.09	0.298	544-601°C	90.62	91.86	Decomposition of the rest ligand and formation of MnO + 5C
[Fe(HL)LCl_2]	Exo	77.15	192.62	1.36	0.57	-0.26	-20.28	0.023	32-205°C	11.58	11.65	Loss of $4CHN_4$
	Exo	197.1	39.25	1.33	0.57	-0.29	-57.49	0.13	77-199°C	46.64	46.6	Loss of $12CH_3OH$, 16 NH_3, 2HCl.
	Exo	268.5	291.32	0.89	0.65	-0.28	-75.21	0.001	199-266°C	60.51	60.61	Loss of $4CH_3SH$, 4 C_2H_5OH
	Exo	340	5.103	1.19	0.59	-0.31	-108	0.016	266-544°C	71.63	71.97	Loss $4C_6H_6$
	Endo	417.1	58.112	1.44	0.56	-0.30085	-125.49	0.016	544-601°C	94.3	94.1	Decomposition of the rest ligand and formation of Fe_2O_3
	Exo	542.8	74.618	0.8	0.67	-0.30315	-164.56	0.298				
[CoL(HL)Cl(H_2O)]	Endo	109.3	61.91	1.73	0.52	-0.27	-30.39	0.06	34-83°C	1.51	1.25	Elimination of H2O
	Endo	202.8	76.8	1.3	0.58	-0.28	-58.12	0.04	83-202°C	10.43	10.65	Elimination of 2NH3,2CH3OH and HCl
	Exo	251.4	210.58	1.74	0.52	-0.28	-70.82	0.1	202-328°C	44.61	44.54	Loss of 2C6H6O, 2CHN4 , 2CH3OH and 2CH3SH
	Endo	385.7	232.56	2.33	0.47	-0.28	-111.08	0.07	328-446.2°C	56.62	55.87	Decomposition of the rest ligand.
[CuLCl(H_2O)]	Endo	122.8	24.04	1.38	0.57	-0.28	-35.36	0.02	34- 202°C	9.75	9.32	Elimination of 2H2O and 3HCl
	Exo	260	31.68	1.18	0.6	-0.29	-77.48	0.01	202 -430°C	51.63	51.73	Loss of 2C6H6O, 2CHN4 , 2CH3COCH3 , 2CH3SH,2NH3 and HCl
	Exo	471.5	66.5	1.11	0.61	-0.3	-142.28	0.01	430- 510°C	89.65	89.16	Decomposition of the rest ligand and formation of 2CuO.

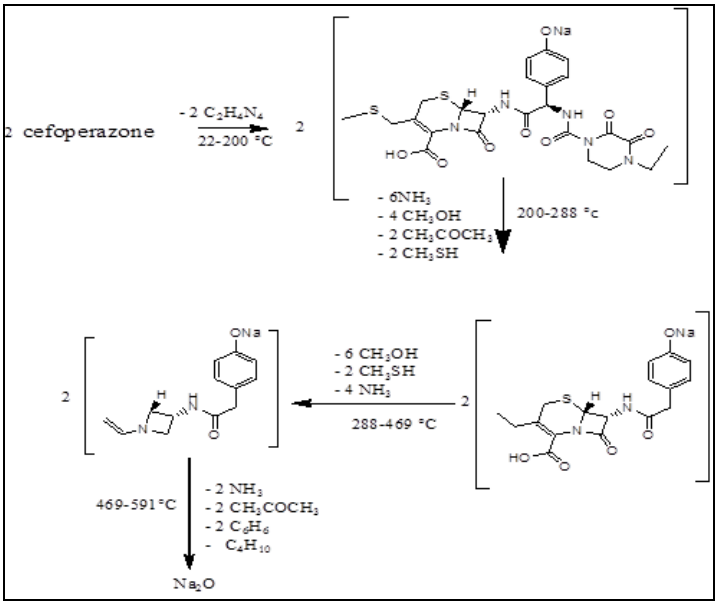

Scheme 1: Thermolysis of cefoperazone ligand

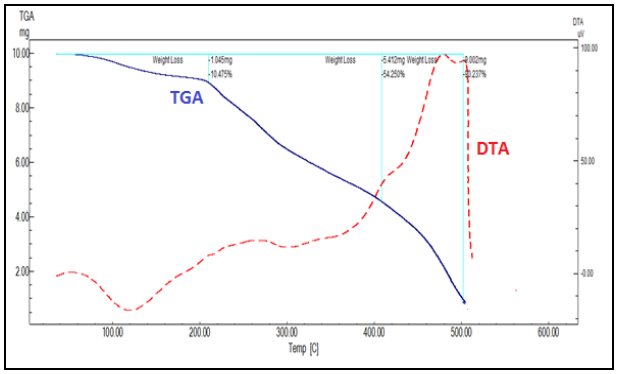

Figure 6: TGA and DTA of Cr- cefoperazone complex

In case of [ZnLCl(H_2O)]complex (Figures 7 anad 8), the first stage of decomposition starts at 25°C and ends at 200°C with a corresponding weight loss 9.39%, which is accompanied by endothermic effect in the DTA curve in the range 123°C which is accompanied by confirmed weight loss. The second stages of decomposition are observed at 280-400°C (52.36% wt loss), meanwhile the DTA curve exhibits exothermic effect in the range 260°C which are accompanied by confirmed weight loss. The last stage of decomposition start at 420°C and ends at 505°C (91.78% wt loss) meanwhile the DTA curve exhibits exothermic effect in the range 471.5°C which is accompanied by confirmed weight loss. The suggested mechanism is given as follows:

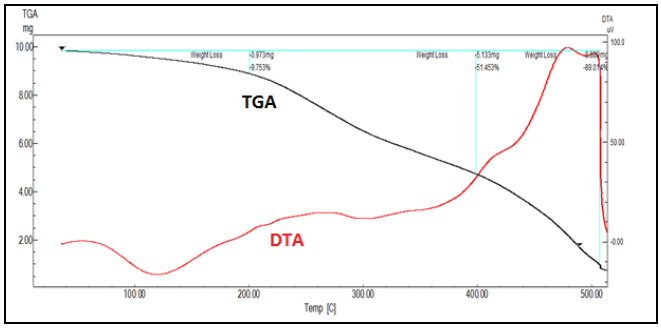

Figure 7: TGA and DTA of Zn- cefoperazone complex

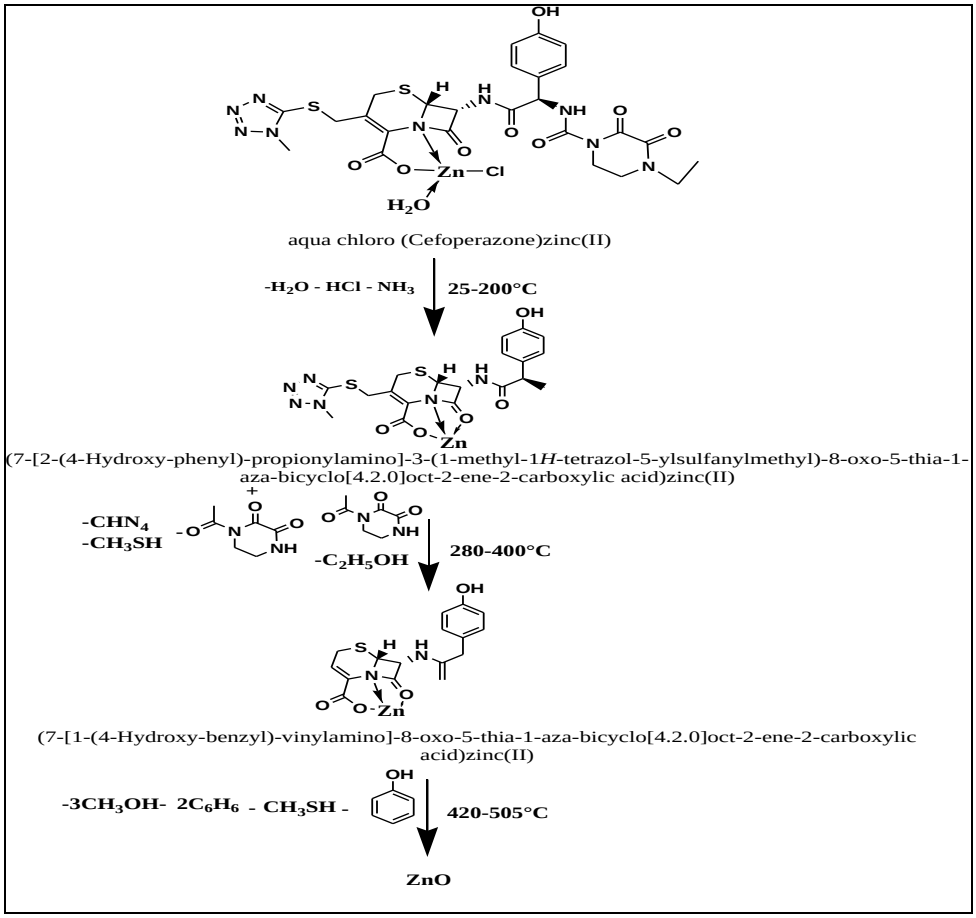

Scheme 2: Thermolysis of [Zn(cefoperazone)Cl (H20)] complex

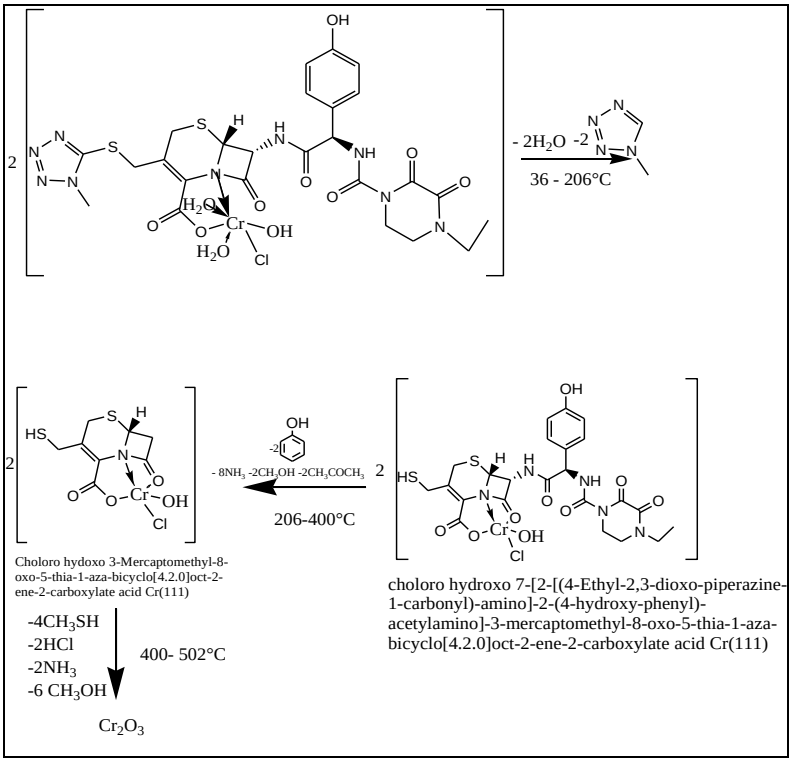

Scheme 3: Thermolysis of [Cr(cefoperazone)(OH)2(Cl)(H20)] complex

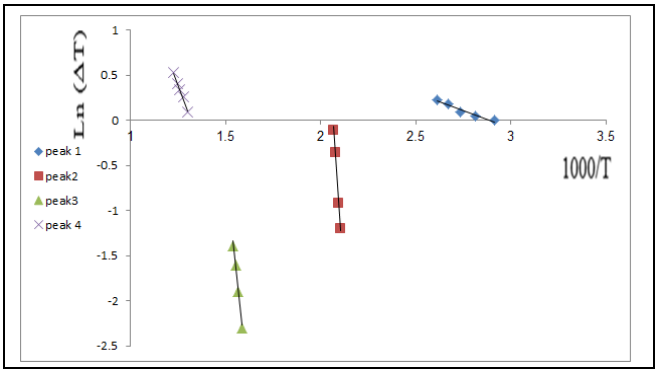

Figure 8: lnΔT against 10^3/T relation for cefoperazone ligand (as a representative figure)

CONCLUSION

Cefoperazone metals complexes are synthesized and characterized by different spectroscopic methods. The complexes formed in different Stoichiometry. All have Oh geometry except for (Ni,Cu and Hg) complexs have tetrahedral geometry and these results confirmed by Nujol and ESR spectra. Cefoperazone act as a bidintate ligand. Also have different sites available for coordination which carries more electronegative charges and the computational study confirms these results. Cefoperazone thermal decomposition is terminated by the formation of carbon residue as a final product. The thermal decomposition of the complexes ended with the formation of metal oxides and carbon residue as a final product except for the case of Hg complex. Thermodynamic parameters such as Ea, ΔH*and ΔS*were estimated from DTA curves. Cefoperazone complexes show higher activity than commercial cefoperazone for some strains.

REFERENCES

[1] SY Essack. *Pharm Res*. **2001**, 18(10), 1391-1399.
[2] AG Gilman; LS Goodman. The Pharmacological Basis of Therapeutics, Macmillan Publishing Company, New York, **1985**.
[3] JR Anacona; A Bravo; ME Lopez. *J Chil Chem Soc*. **2013**, 58, 1520-1523.
[4] AI Vogel. A Text Book of Quantitative Inorganic Analysis, Longmans, London, **1989**.
[5] G Schwarzenbach. Complexometric Titration, Translated by H, Methuen Co., London, Irving, **1957**.
[6] RH Lee; E Griswold; J Kleinberg. *Inorg Chem*. **1964**, 3, 1278-1283.
[7] GB Mohamed; MS Masoud; AM Hindawy; RH Ahmed. *J Pharm Sci*. **1989**, 3(2), 141-145.
[8] MS Masoud; OHA Hamid; ZM Zaki. *Trans Met Chem*. **1994**, 19, 21-24.
[9] K Nakamoto. Infrared and Raman Spectra of Inorganic and Coordination compounds,4th edition, John Wiley, New York, **1986**.
[10] H Zegota; M Koprowski; A Zegota. *Radiat Phys Chem*. **1994**, 43(4), 343-348.
[11] MS Masoud; EA Khalil; O Hamid; AA Soayed. *Egypt Sci Mag*. **2005**, 2(2), 33-37.
[12] MBH Howlader; MS Islam; MR Karim. *Ind J Chem*. **2000**, 39A, 407-409.
[13] A Sreekanth; M Joseph; HK Fun; MRP Kurup. *Polyhedron*. **2006**, 25(6), 1408-1414.
[14] EK Barefield; DH Busch; SM Nelson. *Quart Rev*. **1968**, 22(4), 457- 498.
[15] SJ Kirubavathy; R Velmurugan; K Parameswari; S Chitra. *Int J Pharma Sci Res*. **2014**, 5(6), 2508-2517.
[16] MS Masoud; AE Ali; MA Shaker; GS Elasala. *Spectrochim Acta*. **2012**, A90, 93-108.
[17] MS Masoud; AE Ali; HM Ahmed; EA Mohamed. *J Mol Str*. **2013**, 1050, 43-52.
[18] MS Masoud; AE Ali; GS Elasala. *J Mol Stru*. **2014**, 1084, 259-273.
[19] MS Masoud; AE Ali; GS Elasala. *Spectrochim Acta A*. **2015**, 149, 363-377.
[20] MS Masoud; AE Ali; DA Ghareeb; NM Nasr. *J Mol Str*. **2015**, 1099, 359-372.